

Theory for Tunnel Magnetoresistance Oscillation

Keisuke Masuda,^{1,*} Thomas Scheike,¹ Hiroaki Sukegawa,¹ Yusuke Kozuka,² Seiji Mitani,^{1,3} and Yoshio Miura^{1,4,5}

¹Research Center for Magnetic and Spintronic Materials,
National Institute for Materials Science (NIMS), Tsukuba 305-0047, Japan

²Research Center for Materials Nanoarchitectonics,
National Institute for Materials Science (NIMS), Tsukuba 305-0047, Japan

³Graduate School of Science and Technology, University of Tsukuba, Tsukuba 305-8577, Japan

⁴Faculty of Electrical Engineering and Electronics,
Kyoto Institute of Technology, Matsugasaki, Sakyo-ku, Kyoto, 606-8585, Japan

⁵Center for Spintronics Research Network, Graduate School of Engineering Science,
Osaka University, Toyonaka, Osaka 560-8531, Japan

(Dated: June 13, 2024)

The universal oscillation of the tunnel magnetoresistance (TMR) ratio as a function of the insulating barrier thickness in crystalline magnetic tunnel junctions (MTJs) is a long-standing unsolved problem in condensed matter physics. To explain this, we here introduce a superposition of wave functions with opposite spins and different Fermi momenta, based on the fact that spin-flip scattering near the interface provides a hybridization between majority- and minority-spin states. In a typical Fe/MgO/Fe MTJ, we solve the tunneling problem and show that the TMR ratio oscillates with a period of $\sim 3 \text{ \AA}$ by varying the MgO thickness, consistent with previous and present experimental observations.

The tunneling effect is one of the most fundamental phenomena in quantum mechanics originating from the wave nature of matter. In particular, the quantum tunneling has played an important role for various topics in condensed matter physics. For example, in the case of p - n junctions, electrons tunnel through the depletion layer under large electric field, giving rise to novel negative differential resistance [1]. As another example, tunneling spectrum in a metal/insulator/superconductor junction provides a clear signature of a gap structure in the density of states of the superconductor, validating the Bardeen-Cooper-Schrieffer theory [2]. Moreover, the scanning tunneling microscope utilizes tunneling electrons for imaging surfaces in the atomic level [3].

The tunnel magnetoresistance (TMR) effect is another topic related to the tunneling in the field of spintronics. This occurs in magnetic tunnel junctions (MTJs) consisting of an insulating barrier sandwiched between ferromagnetic electrodes [Fig. 1(a)]. The wave functions in different spin channels have different transmission probabilities because of imbalanced band structures, leading to finite magnetoresistance. One can estimate the magnitude of the magnetoresistance by defining the TMR ratio as a ratio of resistances between parallel and antiparallel magnetization states of the two ferromagnetic electrodes. In 2004, Parkin *et al.* [4] and Yuasa *et al.* [5] reported significantly high TMR ratios in Fe(Co)/MgO/Fe(Co)(001) MTJs, which provided a basis for further fundamental studies of the TMR effect and their device applications.

However, there is a missing piece in the mechanism of such a giant TMR effect; the universal oscillation of the TMR ratio as a function of the insulating barrier thickness [5, 6] has not been explained satisfactorily. In the first report of the giant TMR effect in Fe/MgO/Fe(001) [5], Yuasa *et al.* observed an oscillation of the TMR ra-

tio with a period of $\sim 3 \text{ \AA}$ by varying the MgO thickness, referred to as the “TMR oscillation.” Subsequent experiments [6] clarified that the TMR oscillation originates from resistance oscillations in both the parallel and antiparallel magnetization states. Here, electron tunneling through MgO occurs between the same (different) spin states of the two electrodes in the parallel (antiparallel) magnetization state. Latest experiments for a series of MTJs with high crystallinity [7–9] found that the TMR oscillation with a period of $\sim 3 \text{ \AA}$ is universally observed and its amplitude is much larger than that ever reported. Therefore, to elucidate the origin of the TMR oscillation will advance our understanding not only on the TMR effect but also on the quantum tunneling itself. This will also provide guiding principles for achieving even higher TMR ratios.

Conventionally, high TMR ratios in Fe/MgO/Fe(001) have been explained by the Δ_1 coherent tunneling mechanism; the half-metallic Δ_1 band structure of Fe [Figs. 1(b) and 1(c)] and the slowest decaying Δ_1 evanescent state of MgO enable a selective tunneling of the perfectly spin-polarized Δ_1 state, leading to a high TMR ratio [10, 11]. However, the TMR oscillation cannot be explained by this mechanism [10–12]. Although additional effects, such as interference of evanescent states [10] and nonspecular tunneling [13], have been considered, these provide a resistance oscillation only in the antiparallel magnetization state, qualitatively in disagreement with the experimental results. Another study [14] proposed an oscillation of the TMR ratio due to the quantization in the ferromagnetic layer, but this occurs when varying the thickness of the ferromagnetic layer, inconsistent with the experimental situation.

In this Letter, we show that the TMR oscillation can be explained by taking into account a superposition of

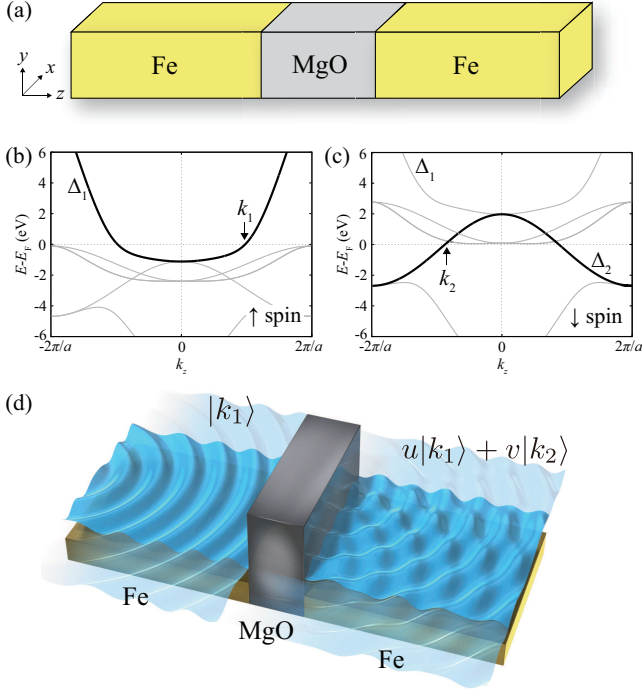


FIG. 1. (a) Schematic of the Fe/MgO/Fe MTJ. (b,c) Majority (\uparrow) -spin and minority (\downarrow) -spin band structures of bcc Fe along the Δ line with $\mathbf{k}_{\parallel} = 0$. (d) Illustration of our idea including a superposition of wave functions with different Fermi momenta.

wave functions with opposite spins and different Fermi momenta for the tunneling problem. It is known that spin-flip scattering occurs near interfaces of MTJs [15–17], indicating that spin is not a good quantum number in this system. This provides a hybridization between majority- and minority-spin states with different Fermi momenta [Figs. 1(b) and 1(c)], which justifies our assumption on the superposition of wave functions. Focusing on Fe/MgO/Fe(001), we solve tunneling problems assuming a superposition of majority-spin Δ_1 and minority-spin Δ_2 wave functions with different Fermi momenta as a transmission wave function [see Fig. 1(d)]. We obtain transmittances in the parallel and antiparallel magnetization states, from which the TMR ratio is calculated. It is found that the transmittances and the TMR ratio have oscillatory behaviors with a period of $\sim 3 \text{ \AA}$ as a function of the MgO thickness, in agreement with previous and present experimental observations. We also show that the calculated TMR ratio can reproduce our experimental results not only qualitatively but also quantitatively by tuning the parameters in our model. Although we focus on the TMR oscillation in this study, the superposition of wave functions with different Fermi momenta is a general concept and would be helpful to understand transport properties in other tunnel junctions with superconductors, semiconductors, etc.

To make the point of our approach clearer, we start from reviewing the conventional analytical treatment of the tunneling problem in an MTJ. Let us consider the situation that the wave function in the left electrode propagates to the right electrode passing through the insulating barrier, which is described by a coordinate system with the z axis along the stacking direction of the MTJ [Fig. 1(a)]. For simplicity, we focus on the wave functions with $\mathbf{k}_{\parallel} = (k_x, k_y) = (0, 0)$ providing the dominant contribution to tunneling transport. When the Fermi momentum is given by $k_z = k_L$ (k_R) in the left (right) electrode, the wave function ψ_L (ψ_R) in the left (right) electrode and the wave function ψ_b in the insulating barrier are expressed as

$$\psi_L = e^{ik_L z} + R e^{-ik_L z}, \quad (1)$$

$$\psi_b = A e^{-\kappa z} + B e^{\kappa z}, \quad (2)$$

$$\psi_R = C e^{ik_R z}, \quad (3)$$

where κ is the decaying wave number inside the insulating barrier. After determining R , A , B , and C from continuation conditions for the wave function and its derivative at $z = 0$ and d , we find the following expression for the transmittance [18]:

$$T = \frac{16 \tilde{k}_L \kappa^2 \tilde{k}_R e^{2\kappa d}}{\left[\kappa (\tilde{k}_L + \tilde{k}_R) (1 + e^{2\kappa d}) \right]^2 + \left[(\kappa^2 - \tilde{k}_L \tilde{k}_R) (1 - e^{2\kappa d}) \right]^2}, \quad (4)$$

where d is the thickness of the insulating barrier, $\tilde{k}_L = (m_b/m_L) k_L$, and $\tilde{k}_R = (m_b/m_R) k_R$. Here, $m_{L(R)}$ and m_b are the effective masses in the left (right) electrode and the insulating barrier, respectively. We can obtain the conductance G by substituting Eq. (4) into the Landauer formula $G = (e^2/h)T$. The Δ_1 coherent tunneling mechanism mentioned above can be confirmed by employing this tunneling theory in combination with the first-principles calculation [19–21].

However, this conventional tunneling theory cannot describe the oscillation of the TMR ratio in the Fe/MgO/Fe(001) MTJ. Actually, the transmittance in the parallel magnetization state is obtained by putting $k_L = k_R = k_1$ (or k_2) in Eq. (4), where k_1 and k_2 are the Fermi momenta of the majority-spin Δ_1 and the minority-spin Δ_2 bands of Fe, respectively [see Figs. 1(b) and 1(c)]. Note that the negative k_2 value with a positive group velocity is chosen for the minority-spin state, since we focus on right-moving states. The transmittance in the antiparallel magnetization state is similarly obtained by setting $k_L = k_1$ (or k_2) and $k_R = k_2$ (or k_1) in Eq. (4). As seen from Eq. (4), both the parallel and antiparallel transmittances decrease exponentially with increasing d in monotonic manner without any oscillations.

To explain the oscillation in the transmittance, we introduce a superposition of wave functions between the

majority-spin Δ_1 and minority-spin Δ_2 states for the transmission wave in the tunneling problem. This is justified due to the existence of spin-flip scattering at interfaces, as mentioned in the introduction. Let us first calculate the parallel transmittance T_P . Based on the fact that the majority-spin Δ_1 state provides the dominant contribution to the TMR effect [10, 11], T_P can be calculated as $T_P = T_{P,\uparrow} + T_{P,\downarrow} \approx T_{P,\uparrow}$, where \uparrow (\downarrow) indicates that tunneling electrons are in the majority-spin (minority-spin) state in the left electrode. For the calculation of $T_{P,\uparrow}$, we consider a tunneling from the majority-spin Δ_1 state in the left electrode to the superposition state in the right electrode with the dominant contribution from the majority-spin Δ_1 state, which is given by

$$\psi_L = e^{ik_1 z} + R e^{-ik_1 z}, \quad (5)$$

$$\psi_b = A e^{-\kappa z} + B e^{\kappa z}, \quad (6)$$

$$\psi_R = C (u e^{ik_1 z} + v e^{ik_2 z}). \quad (7)$$

Here, u and v are matrix elements of the unitary matrix that diagonalizes the 2×2 Hamiltonian in the spin space with off-diagonal elements. The off-diagonal elements reflect the existence of spin-flip scattering at interfaces. Although we do not specify the expressions of u and v , these can be given by some types of many-body interactions leading to spin-flip scattering, e.g., the s - d exchange interaction at interfaces [17]. We impose $|u| \gg |v|$ because of the dominance of the majority-spin Δ_1 state in $T_{P,\uparrow}$. The matrix elements also satisfy the normalization condition $|u|^2 + |v|^2 = 1$. By using the continuity of the wave function and its derivative at $z = 0$ and d , we can derive the following expression for $T_{P,\uparrow}$:

$$T_{P,\uparrow} = \tilde{k}_{1L}^{-1} \left[\tilde{u}^2 \tilde{k}_{1R} + \tilde{v}^2 \tilde{k}_{2R} + \tilde{u}\tilde{v} (\tilde{k}_{1R} + \tilde{k}_{2R}) \cos((k_1 - k_2)d - \theta) \right] |C|^2, \quad (8)$$

$$\begin{aligned} \text{Denominator of } |C|^2 &= (e^{\kappa d} - e^{-\kappa d})^2 \left\{ \kappa^4 [1 + 2\tilde{u}\tilde{v} \cos((k_1 - k_2)d - \theta)] \right. \\ &\quad - 2\kappa^2 \tilde{k}_{1L} \left[\tilde{u}^2 \tilde{k}_{1R} + \tilde{v}^2 \tilde{k}_{2R} + \tilde{u}\tilde{v} (\tilde{k}_{1R} + \tilde{k}_{2R}) \cos((k_1 - k_2)d - \theta) \right] \\ &\quad \left. + \tilde{k}_{1L}^2 \left[\tilde{u}^2 \tilde{k}_{1R}^2 + \tilde{v}^2 \tilde{k}_{2R}^2 + 2\tilde{u}\tilde{v} \tilde{k}_{1R} \tilde{k}_{2R} \cos((k_1 - k_2)d - \theta) \right] \right\} \\ &\quad + (e^{\kappa d} + e^{-\kappa d})^2 \left\{ \kappa^2 \tilde{k}_{1L}^2 [1 + 2\tilde{u}\tilde{v} \cos((k_1 - k_2)d - \theta)] \right. \\ &\quad \left. + 2\kappa^2 \tilde{k}_{1L} \left[\tilde{u}^2 \tilde{k}_{1R} + \tilde{v}^2 \tilde{k}_{2R} + \tilde{u}\tilde{v} (\tilde{k}_{1R} + \tilde{k}_{2R}) \cos((k_1 - k_2)d - \theta) \right] \right. \\ &\quad \left. + \kappa^2 \left[\tilde{u}^2 \tilde{k}_{1R}^2 + \tilde{v}^2 \tilde{k}_{2R}^2 + 2\tilde{u}\tilde{v} \tilde{k}_{1R} \tilde{k}_{2R} \cos((k_1 - k_2)d - \theta) \right] \right\} \\ &\quad + 2(e^{\kappa d} + e^{-\kappa d})(e^{\kappa d} - e^{-\kappa d}) \tilde{u}\tilde{v} (\kappa^2 + \tilde{k}_{1L}^2) \kappa (\tilde{k}_{1R} - \tilde{k}_{2R}) \sin((k_1 - k_2)d - \theta) \quad (9) \\ \text{Numerator of } |C|^2 &= 16 \tilde{k}_{1L}^2 \kappa^2, \quad (10) \end{aligned}$$

where $\tilde{k}_{1L} = (m_b/m_L)k_1$, $\tilde{k}_{1R} = (m_b/m_R)k_1$, and $\tilde{k}_{2R} = (m_b/m_R)k_2$. We put $u = \tilde{u}$ and $v = \tilde{v} e^{i\theta}$ using positive real numbers \tilde{u} and \tilde{v} . The relation $\tilde{u}^2 + \tilde{v}^2 = 1$ was used to simplify the expression. Equations (8) and (9) include several terms with $\cos((k_1 - k_2)d - \theta)$ or $\sin((k_1 - k_2)d - \theta)$, leading to an oscillation of the transmittance as a function of d . The antiparallel transmittance $T_{AP,\uparrow}$ is easily obtained by replacing \tilde{u} with \tilde{v} and \tilde{v} with $-\tilde{u}$ in Eqs. (8)-(10). Since $\tilde{u} \gg \tilde{v}$, this replacement allows us to consider the transmittance for the electron tunneling from the majority-spin Δ_1 state in the left electrode to the superposition state in the right electrode with the dominant contribution from the minority-spin Δ_2 state, which corresponds to $T_{AP,\uparrow}$. Using $T_{AP,\uparrow}$, the total antiparallel transmittance can be calculated as $T_{AP} = T_{AP,\uparrow} + T_{AP,\downarrow} \approx 2T_{AP,\uparrow}$. We simply set $\tilde{u} = 0.95$, $\theta = 0$, $m_b/m_L = 1.0$, and $m_b/m_R = 1.0$ (-1.0) for the numerical calculation of $T_{P,\uparrow}$ ($T_{AP,\uparrow}$); however, the choice of these parameters hardly affects the qualitative features of oscillations in transmittances. Note here that m_b/m_L

and m_b/m_R need to have different signs in the antiparallel state, since Δ_1 and Δ_2 bands have different signs of effective masses as seen from Figs. 1(b) and 1(c).

Figure 2 shows inverses of parallel and antiparallel transmittances, $T_{P,\uparrow}^{-1}$ and $T_{AP,\uparrow}^{-1}$, divided by the exponentially increasing factor $\exp(2\kappa d)$. Here, we set $\kappa = 0.2\pi/a_{\text{MgO}}$ ($a_{\text{MgO}} = 4.217 \text{ \AA}$: lattice constant of MgO), which is the decaying wave number for the Δ_1 complex band of MgO calculated by the PWCOND code [22]. We also used $k_1 = 1.0\pi/a_{\text{Fe}}$ and $k_2 = -0.9\pi/a_{\text{Fe}}$ ($a_{\text{Fe}} = 2.866 \text{ \AA}$: lattice constant of bcc Fe) obtained by calculating the band structure of bcc Fe [Figs. 1(b) and 1(c)] with the aid of QUANTUM ESPRESSO [23]. In both $T_{P,\uparrow}^{-1}$ and $T_{AP,\uparrow}^{-1}$, we can see a clear oscillation with a period of $2\pi/(k_1 - k_2)$. From the values of k_1 and k_2 mentioned above, the period is estimated to be $\sim 3 \text{ \AA}$. These are consistent with the experimental fact that resistances in both the parallel and antiparallel magnetization states have oscillatory barrier thickness dependences with periods of $\sim 3 \text{ \AA}$ [6, 8, 9]. In addition, a finite phase difference

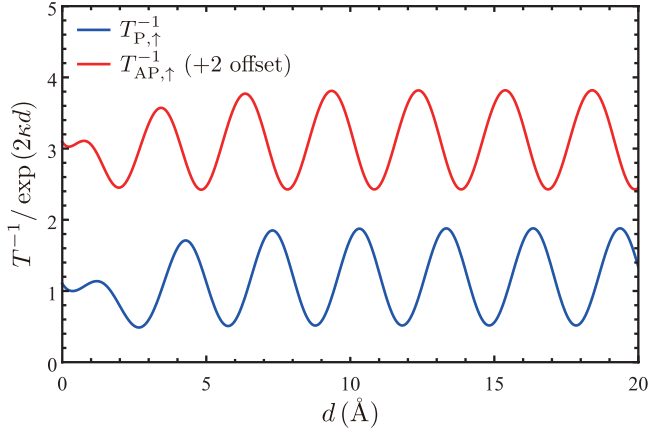


FIG. 2. Barrier thickness d dependences of inverses of parallel and antiparallel transmittances, $T_{P,\uparrow}^{-1}$ and $T_{AP,\uparrow}^{-1}$, divided by $\exp(2\kappa d)$.

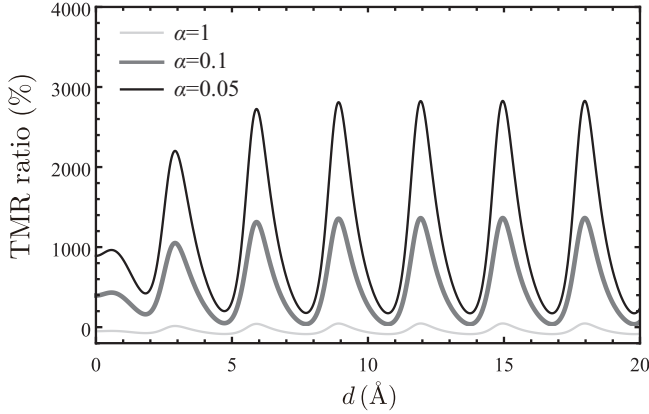


FIG. 3. TMR ratios as a function of the barrier thickness d for different values of α . This was obtained by Eq. (11).

between $T_{P,\uparrow}^{-1}$ and $T_{AP,\uparrow}^{-1}$ can be seen in Fig. 2, which is essential for the occurrence of the TMR oscillation discussed below.

By using $T_{P,\uparrow}$ and $T_{AP,\uparrow}$, we calculated the TMR ratio given by

$$(T_P - \alpha T_{AP}) / \alpha T_{AP} \approx (T_{P,\uparrow} - 2\alpha T_{AP,\uparrow}) / 2\alpha T_{AP,\uparrow}, \quad (11)$$

where α is an adjustment parameter between T_P and T_{AP} . Figure 3 shows barrier thickness d dependences of the TMR ratio for different values of α . For all the values of α , the TMR ratio shows an oscillation with a period of $2\pi/(k_1 - k_2) \sim 3 \text{ \AA}$ similarly to $T_{P,\uparrow}^{-1}$ and $T_{AP,\uparrow}^{-1}$. The parameter α is set to 1 in the usual definition of the TMR ratio. However, the TMR ratio takes negative values for $\alpha = 1$, inconsistent with positive high TMR ratios observed in experiments. This is because the present analysis employs only the values of the Fermi momenta and the decaying wave number and does not consider detailed electronic structures of bcc Fe and MgO. If the electronic structures are taken into account by using the

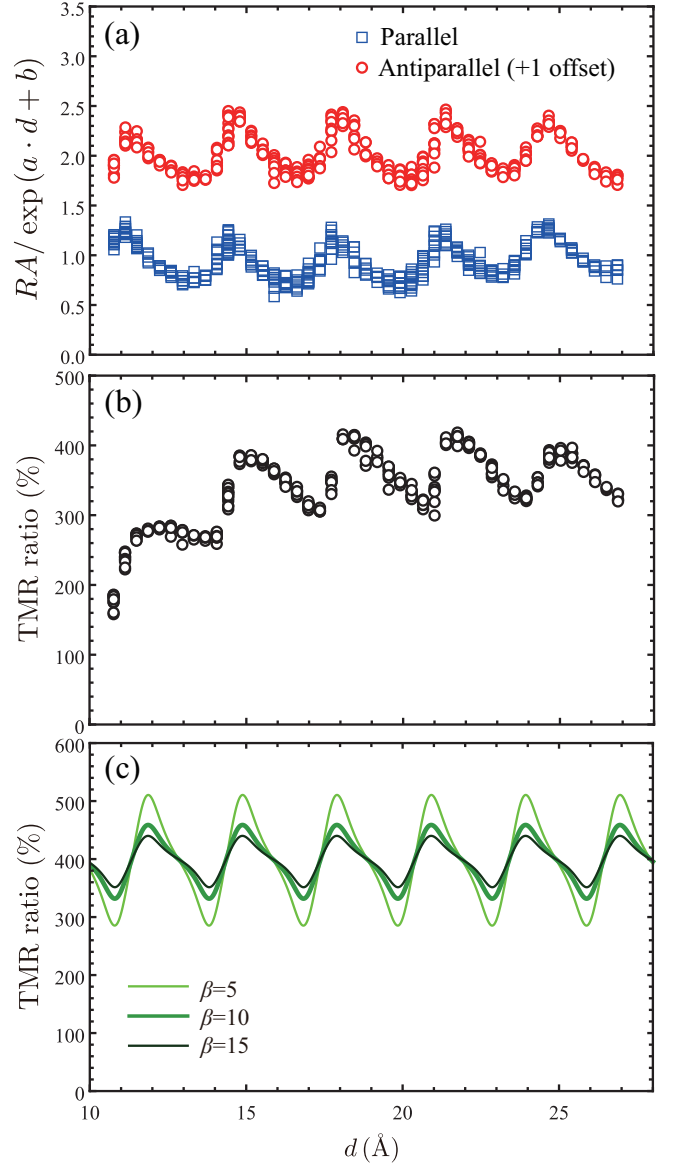


FIG. 4. Experimental results of (a) RA values and (b) TMR ratios in $\text{Fe}/\text{Mg}_4\text{AlO}_x/\text{Fe}(001)$ at room temperature. (c) Theoretical values of TMR ratios for different values of β calculated by Eq. (12) with $\alpha = 0.1$.

first-principles calculation [10, 11], values of T_{AP} should be much smaller than those of T_P . Thus, we hereafter set $\alpha = 0.1$ for a better comparison with experimental values of the TMR ratio obtained at room temperature [24].

Finally, let us directly compare our calculation results with an experimentally observed TMR oscillation. To this aim, we fabricated a MTJ structure and measured magnetotransport properties. The experimental details are explained in the Supplemental Material. Figure 4(a) shows barrier thickness d dependences of the resistance-area product (RA) in the parallel and antiparallel magnetization states, where RA is a product of the resistance

and the cross-sectional area of the MTJ. We show values of the RA divided by $\exp(a \cdot d + b)$, where a and b were determined to be 5.48 (5.73) nm^{-1} and -2.36 (-1.35) in the parallel (antiparallel) magnetization state, respectively, from the fits using the exponential function. As seen in Fig. 4(a), the RA has an oscillatory d dependence with a period of 3.1 \AA in both the parallel and antiparallel magnetization states. Since there is a finite phase difference in RA values between the parallel and antiparallel magnetization states, the TMR ratio has a similar oscillation as shown in Fig. 4(b). For a direct comparison with our experimental results, we introduced another parameter β for non-oscillatory components [25] and calculated the TMR ratio given by

$$[(T_P + \beta e^{-2\kappa d}) - \alpha (T_{AP} + \beta e^{-2\kappa d})] / \alpha (T_{AP} + \beta e^{-2\kappa d}), \quad (12)$$

where α is fixed to 0.1 as mentioned above. Note here that our present theory focuses on the electronic state along the Δ line just at $\mathbf{k}_{\parallel} = 0$ because of its dominant contribution to the TMR effect. However, in actual experiments, electronic states around $\mathbf{k}_{\parallel} = 0$ can also contribute to the transmission, which can justify the inclusion of β in our expression. Figure 4(c) shows the calculated TMR ratios for different values of β . The shape of the TMR oscillation is quite similar to that in our experimental results, which show a saw-tooth like oscillation [26]. In addition, the TMR ratios calculated for $\beta = 10$ are found to quantitatively agree with experimental values. Therefore, we conclude that the TMR ratio calculated by Eq. (12) can reproduce the experimental results not only qualitatively but also quantitatively.

In summary, we proposed a theory for explaining the universal oscillation of the TMR ratio called the ‘‘TMR oscillation.’’ Based on the fact that spin-flip scattering occurs near interfaces of MTJs, we took into account the superposition of the majority-spin Δ_1 and minority-spin Δ_2 wave functions with different Fermi momenta for the tunneling problem in Fe/MgO/Fe(001). We analytically calculated transmittances in the parallel and antiparallel magnetization states, from which the TMR ratio was obtained. It was found that the transmittances and the TMR ratio have oscillatory barrier thickness dependences with a period of $\sim 3 \text{ \AA}$, consistent with the experimental observations. According to our theory, the period of the TMR oscillation is determined by the difference of the Fermi momenta between the majority- and minority-spin states in the ferromagnetic electrode. Therefore, the period of $\sim 3 \text{ \AA}$ is specific to bcc Fe used as electrodes. If MTJs with other ferromagnetic electrodes are successfully made, TMR oscillations with periods different from 3 \AA would be observed. We can also predict that a resistance oscillation cannot be observed in tunnel junctions with nonmagnetic electrodes, since the spin degree of freedom is essential for the resistance oscillation in our theory. We expect future experimental studies using a

wider range of materials will provide further information for the TMR oscillation.

The authors are grateful to S. Yuasa for fruitful discussions. This work was supported by Grants-in-Aid for Scientific Research (Grant Nos. 22H04966, 23K03933, and 24H00408) and MEXT Program: Data Creation and Utilization-Type Material Research and Development Project (Grant No. JPMXP1122715503). MANA is supported by the World Premier International Research Center Initiative (WPI) of MEXT, Japan. The band structure calculation was performed on the Numerical Materials Simulator at NIMS.

* MASUDA.Keisuke@nims.go.jp

- [1] L. Esaki, Phys. Rev. **109**, 603 (1958).
- [2] I. Giaever, Phys. Rev. Lett. **5**, 147 (1960).
- [3] G. Binnig and H. Rohrer, Rev. Mod. Phys. **59**, 615 (1987).
- [4] S. S. P. Parkin, C. Kaiser, A. Panchula, P. M. Rice, B. Hughes, M. Samant, and S.-H. Yang, Nat. Mater. **3**, 862 (2004).
- [5] S. Yuasa, T. Nagahama, A. Fukushima, Y. Suzuki, and K. Ando, Nat. Mater. **3**, 868 (2004).
- [6] R. Matsumoto, A. Fukushima, T. Nagahama, Y. Suzuki, K. Ando, and S. Yuasa, Appl. Phys. Lett. **90**, 252506 (2007).
- [7] T. Scheike, Q. Xiang, Z. Wen, H. Sukegawa, T. Ohkubo, K. Hono, and S. Mitani, Appl. Phys. Lett. **118**, 042411 (2021).
- [8] T. Scheike, Z. Wen, H. Sukegawa, and S. Mitani, Appl. Phys. Lett. **120**, 032404 (2022).
- [9] T. Scheike, Z. Wen, H. Sukegawa, and S. Mitani, Appl. Phys. Lett. **122**, 112404 (2023).
- [10] W. H. Butler, X.-G. Zhang, T. C. Schulthess, and J. M. MacLaren, Phys. Rev. B **63**, 054416 (2001).
- [11] J. Mathon and A. Umerski, Phys. Rev. B **63**, 220403(R) (2001).
- [12] C. Heiliger, P. Zahn, B. Y. Yavorsky, and I. Mertig, Phys. Rev. B **77**, 224407 (2008).
- [13] X.-G. Zhang, Yan Wang, and X. F. Han, Phys. Rev. B **77**, 144431 (2008).
- [14] G. Autès, J. Mathon, and A. Umerski, Phys. Rev. B **84**, 134404 (2011).
- [15] P. Mavropoulos, M. Lezaic, and S. Blügel, Phys. Rev. B **72**, 174428 (2005).
- [16] Y. Miura, K. Abe, and M. Shirai, Phys. Rev. B **83**, 214411 (2011).
- [17] K. Masuda, T. Tadano, and Y. Miura, Phys. Rev. B **104**, L180403 (2021).
- [18] J. M. MacLaren, X.-G. Zhang, and W. H. Butler, Phys. Rev. B **56**, 11827 (1997).
- [19] Y. Miura, S. Muramoto, K. Abe, and M. Shirai, Phys. Rev. B **86**, 024426 (2012).
- [20] K. Masuda and Y. Miura, Jpn. J. Appl. Phys. **56**, 020306 (2017).
- [21] K. Masuda and Y. Miura, Phys. Rev. B **96**, 054428 (2017).
- [22] A. Smogunov, A. Dal Corso, and E. Tosatti, Phys. Rev. B **70**, 045417 (2004).

- [23] P. Giannozzi, S. Baroni, N. Bonini, M. Calandra, R. Car, C. Cavazzoni, D. Ceresoli, G. L. Chiarotti, M. Cococcioni, I. Dabo, A. Dal Corso, S. de Gironcoli, S. Fabris, G. Fratesi, R. Gebauer, U. Gerstmann, C. Gougoussis, A. Kokalj, M. Lazzeri, and L. Martin-Samos et al., *J. Phys.: Condens. Matter* **21**, 395502 (2009).
- [24] TMR ratios at low temperature are more than twice as high as those at room temperature and can be reproduced by using a smaller value of α .
- [25] The non-oscillatory components decrease exponentially as the barrier thickness increases similarly to the oscillatory component, which is expressed by $\beta e^{-2\kappa d}$.
- [26] Experimentally, the shape of the TMR oscillation is different for different samples. Actually, Mg_4AlO_x -based MTJs have saw-tooth like shapes [8] similarly to our present results, while MgO-based MTJs have sine-like shapes [7, 9]. These different shapes can be reproduced by tuning the parameters in our model.